EAI Endorsed Transactions
on Energy Web
Research Article EAI.EU

Optimization design of heliostat field based on high-dimensional particle swarm and multiple population genetic algorithms

Yiwen Huang[1,*]

Southeast University, 2 Sipailou Drive, Nanjing, China

Abstract

INTRODUCTION: Tower-type heliostat field is a new type of energy conversion, which has the advantages of high energy efficiency, flexibility and sustainability and environmental friendliness.
OBJECTIVES: Through the research and improvement of the tower heliostat field to promote the development of solar energy utilization technology.
METHODS: In this paper, we calculate and optimize the tower heliostat field by using single objective optimization, high-dimensional particle swarm algorithm and multiple group genetic algorithm.
RESULTS: In this case of question setting, average annual optical efficiency is 0.6696; average annual cosine efficiency is 0.7564; annual average shadow occlusion efficiency is 0.9766; average annual truncation efficiency is 0.9975; average annual output thermal power is 35539.1747W; mean annual output thermal power per unit area is 0.5657W.The optimal solution after the initial optimization of the algorithm is that the total number of mirror fields is 6,384 pieces, and the average annual output power per unit area is 530.6W.
CONCLUSION: The model of this paper can reasonably solve the problem and has strong practicability and high efficiency, but high dimensional particle swarm algorithm due to easily get local optimal solution, so can introduce the chaotic mapping to increase the randomness of the search space, improve the global search ability of the algorithm.

Keywords: Single-objective optimization; high-dimensional particle swarm algorithm; multiple group genetic algorithm; ray tracing

Received on 29 December 2023, accepted on 29 March 2024, published on 05 April 2024

doi: 10.4108/ew.5653

*Corresponding author. Email: 2431716553@qq.com

1. Introduction

A heliostat is an optical device that reflects the light of the sun or other celestial objects in a fixed direction.

Figure 1. A Schematic diagram of the circular heliostat field[1]

In the heliostat field, different parameters such as heliostat number, layout, absorber position and so on will

have different effects on the output efficiency of the heliostat field. Based on the above background, this paper carries out the calculation and optimization of the tower heliostat field by using single-objective optimization, high-dimensional particle swarm algorithm, multiple group genetic algorithm, etc. The task to be studied in this paper is:

Calculate the annual average optical efficiency and annual average output thermal power of the helioscope field according to the given formula[2] and method model.

When only limit the helioscope field distribution range and absorption tower structure, helioscope size range is the same, design parameters make the field of the rated power, the annual average output thermal power to the maximum, and calculate the annual average optical efficiency, annual output thermal power, and the annual average output thermal power per unit mirror area.

Through the research and improvement of the tower heliostat field, the development of solar energy utilization technology can be promoted, and the application and promotion of renewable energy can be promoted.

2. Problem Preset And Preliminary Analysis

2.1. Problem Presets

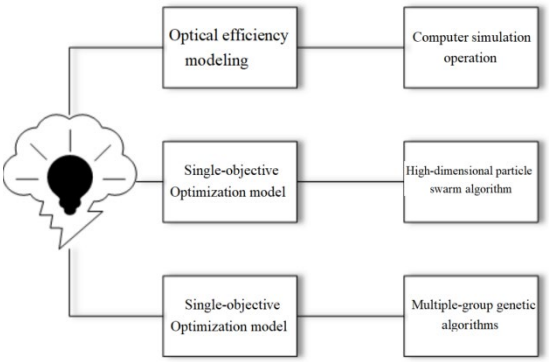

Figure 2. Problem analysis ideas

It is now planned to build a circular heliostat field in the circular area of 98.5 degrees east longitude, 39.4 degrees north latitude, 3000 m elevation and a radius of 350 m. The height of the planned absorption tower is 80 m, and the collector adopts a cylindrical outer light collector with a height of 8 m and a diameter of 7 m. No helichoscope is installed within 100 m around the absorption tower. The side length of the mirror is between 2 m and 8 m, and the mounting height is between 2 m and 6 m. The mounting height must ensure that the mirror does not touch the ground when rotating around the horizontal axis. Due to the need for maintenance and cleaning of the vehicle, the distance between the center of the adjacent heliostat base is more than 5 m more than the width of the mirror. To simplify the calculation, the calculation points of all "annual" indicators in this problem are 9:00,10:30,12:00,13:30 and 15:00 on the 21st of each month.

According to the design requirements, the rated annual average output thermal power of the helioscope field is 60 MW. If the size of the heliostat can be different and the installation height can be different, please design the following parameters of the heliostat field: the position coordinate of the absorption tower, the size of the heliostat, the installation height, the number of heliostats, and the position of the heliostat, so that the average annual output thermal power per unit mirror area is as large under the rated power as possible.

2.2. Analysis of Problem

First, the solar height Angle, azimuth Angle and radiation irradiance are calculated according to the formula, and then the optical efficiency is calculated. Among them, the shadow occlusion efficiency is calculated by means of Monte Carlo ray tracing and coordinate vector transformation, and the loss value is obtained by calculating the intersection area by dividing the mirror grid points. Cosine efficiency is more intuitive, and it can be obtained only by using the quantity product of the unit mirror normal vector and the unit reflection vector. The truncation efficiency of the collector is calculated using the integral equation of the energy flow density, approximated to the Gaussian distribution. Atmospheric transmission is only related to the distance from the mirror center to the center of the collector. The mirror reflectivity value is: 0.92. By multiplying all efficiencies, the average annual optical efficiency of the problem mirror field is 66.96%.

2.3. Model Hypothesis

- Suppose that all the formula definitions given in the topic are reasonable and reliable.
- Suppose that the center of the mirror overlaps with the central axis of the heliostat column.
- Suppose that the absorption tower can be positioned anywhere in a circular area with a radius of 100m.
- Suppose that the effect caused by weather is within the allowable range of the atmospheric transmission calculation formula and the error of the distribution law.
- Suppose that the helioscope field is an ideal flat ground at the same altitude with no extra shelter.
- Suppose that the effect of the tapered light is negligible when the cosine efficiency is calculated.
- Suppose that the year is a flat year or regardless of the impact of different days in leap years.

3. Model of Calculation For the Efficiency Parameters

A single objective optimization model is built with the maximum annual average output thermal power per unit mirror area as the objective function, and the size range of the helichoscope and the coordinate range of the absorber as the constraints. The decision variables are the mirror width, mirror height, installation height and the position coordinates of the absorber, and the size of the heliostat can be inconsistent. Finally, the number of mirror pieces in the mirror field is 4105, and the average annual output thermal power per unit mirror area is 5.306×10-4 MW, which is 0.606×10-4 MW more than the former optimization result.The annual optical efficiency of the heliostat field reflects the efficiency of the heliostat field in converting solar energy into thermal energy. It is known that the mirror surface material affects the reflection performance of the mirror surface. Dust accumulation in the air affects the reflection performance of the mirror surface. The sun's rays will be lost during their propagation. There is a cosine loss between the mirror and the solar incident line. Specular reflection of sunlight will attenuate when it propagates in the atmosphere. The distance causes shadow occlusion between the heliostats. The light reflected by the heliostat is blocked by other heliostats and the light reflected by the heliostat to the collector overflows. It can be seen from the analysis that the optical efficiency index of the heliostatic field should be considered: mirror reflectivity, cosine efficiency, atmospheric transmission efficiency, shadow light blocking efficiency and overflow efficiency.

3.1. Mirror Reflectivity

According to reference [3], in order to ensure that the heliostat can work efficiently, the heliostat must meet the mirror reflectivity greater than 90%. Heliostat material is mainly divided into two kinds. The one is stainless steel and other metal material, whose structure is complex and reflectivity is low, and not used on a large scale. The other is made of glass, whose internal strength is low, and reflectivity is high. Each tower solar power station mainly use this kind of heliostat. Its mirror reflectance is generally 92%~94%. The mirror reflectivity was 92% in this paper.

3.2. Cosine Efficiency

The main reason for the loss of cosine efficiency is that the actual lighting area of the mirror surface is smaller than the mirror area. The sun's incident light reflects the light onto the collector through a mirror. Therefore, there is an Angle θ between the heliostat mirror and the incident light, which is shown in Figure 3.

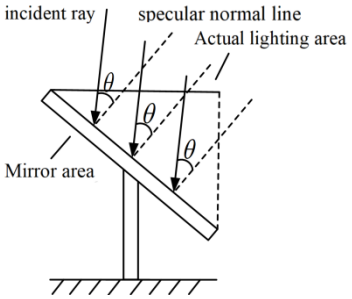

Figure 3. Schematic diagram of the circular heliostat field

As shown in Figure 3, the ratio of the actual lighting area of the heliostat to the mirror area of the heliostat is the cosine efficiency, and its size is related to the clip angle θ. Therefore, the equivalent concentrating schematic diagram of the heliostat is made on the basis of the mirror field coordinate system given by the title, as shown in Figure 4.

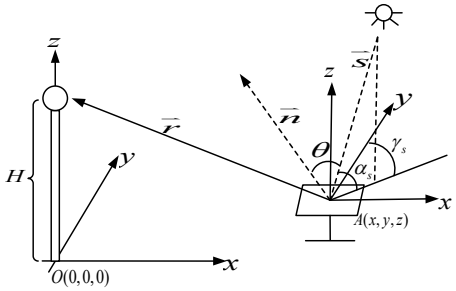

Figure 4. Schematic of heliophograph

As shown in Figure 4, the unit vector of the solar incident rays is $\vec{s}$. The mirror normal vector of the heliostat is $\vec{n}$. The unit vector of the reflected light of the heliostat is $\vec{r}$. The collector coordinates on the absorption tower are P (0,0,H). The coordinates of the center of the heliostat are (x,y,z). Its effective reflection area is:

$$A = \cos[\arccos(\vec{s} \cdot \vec{r})/2] \cdot (LH \cdot LW) \quad (1)$$

Therefore, the cosine efficiency calculation formula is follows:

$$\eta_{COS} = \cos[\arccos(\vec{s} \cdot \vec{r})/2] \quad (2)$$

$$\vec{s} = (-cos\alpha_s sin\gamma_s, -cos\alpha_s cos\gamma_s, -sin\alpha_s) \quad (3)$$

$$\vec{r} = (-x, -y, H-z)/\sqrt{x^2+y^2+(H-z)^2} \quad (4)$$

Solar elevation α_s:

$$\sin\alpha_s = \cos\delta\cos\varphi\cos\omega + \sin\delta \quad (5)$$

Solar azimuth γ_s:

$$\cos\gamma_s = \frac{\sin\delta - \sin\alpha_s \sin\varphi}{\cos\alpha_s \cos\varphi} \quad (6)$$

Among it, φ is local latitude, and north latitude is positive. ω is solar hour angle.

$$\omega = \frac{\pi}{12}(ST - 12) \quad (7)$$

Among it, ST is local time, and δ is the declination angle of the sun.

$$\sin\delta = \sin\frac{2\pi D}{365}\sin(\frac{2\pi}{365}23.45) \quad (8)$$

Among it, D is the number of days from day 0 with the spring equinox as the starting day. For example, if the equinox is March 21, then April 1 represent that D is equal to 11.

3.3. Atmospheric Transmission Efficiency

The main reason for the loss of atmospheric transmission efficiency is that the heliostat reflected solar light is influenced by the atmosphere in the Earth during its propagation, Such as the absorption and scattering of light by the atmosphere. The atmospheric transmission rate is the ratio of the solar light received by the collector to the reflected solar light generated by the heliostat field. The atmospheric transmission efficiency is[2]

$$\eta_{at} = \begin{cases} 0.99321 - 0.0001176d + 1.97 \cdot 10^{-8}d^2, & d \le 1000m \\ exp(-0.0001106d), & d > 1000m \end{cases} \quad (9)$$

Among it, d represents the distance between the mirror center to the collector center.

3.4. Shadow Light Blocking Efficiency

The main reason for the loss of the efficiency of shadow light blocking is that the heliostat in the heliostat field exists where the solar incident line is blocked by other heliostats or the solar light reflected by the heliostat is blocked by other heliostats and cannot be focused to the aggregation tower, which are called shadow loss and occlusion loss. The detailed calculation steps are:

(i) According to the longitude and time of the location, we can calculate the unit vector of the solar incident line $\vec{s}$, unit normal vector of heliostat 1 $\overrightarrow{n_1}$ and unit normal vector of heliostat 2 $\overrightarrow{n_2}$.

(ii) Take the center of the heliostat as the point $O_1 = (x_{O1}, y_{O1}, z_{O1})$, and calculate the vertex coordinates of heliostat 1 as $T_{11}, T_{12}, T_{13}, T_{14}$. The schematic diagram of each space space in the plane is shown in Figure 5. As shown in Figure 5, the vertex coordinates of the heliostat can be obtained according to its geometric relationship. Take T_{13} for example:

$$\begin{cases} x_{T13} = x_{o1} - \frac{1}{2}LW \times \frac{y_{n1}}{\sqrt{x_{n1}^2 + y_{n1}^2}} - \frac{1}{2}LH \times z_{n1} \times \frac{x_{n1}}{\sqrt{x_{n1}^2 + y_{n1}^2}} \\ y_{T13} = y_{o1} - \frac{1}{2}LH \times z_{n1} \times \frac{y_{n1}}{\sqrt{x_{n1}^2 + y_{n1}^2}} + \frac{1}{2}LW \times \frac{x_{n1}}{\sqrt{x_{n1}^2 + y_{n1}^2}} \\ z_{T13} = z_{o1} + \frac{1}{2}LH \times \sqrt{1 - z_{n1}^2} \end{cases} \quad (10)$$

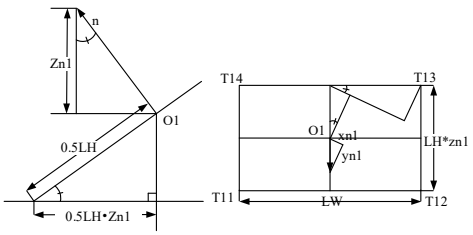

Figure 5. Schematic diagram of spatial coordinates in the heliostat plane

(iii) Calculate the distance between the vertex coordinates of the helioat 1 and the plane of the heliostat 2. Take T_{13} for example:

$$x_{n2}x_{O2} + y_{n2}y_{O2} + z_{n2}z_{O2} + D_2 = 0 \quad (11)$$

From this, it can be deduced:

$$x_{n2}x_{T13} + y_{n2}y_{T13} + z_{n2}z_{T13} + D_{T13} = 0 \quad (12)$$

Thus, the plane distance from the vertex to heliostat 2 in the direction of the incident solar rays is:

$$L_3 = \left|\frac{D_2 - D_{T13}}{\overrightarrow{n_2} \cdot \vec{s}}\right| \quad (13)$$

(iv) The heliostat vertex coordinates obtained in previous step are projected to the heliostat 2 plane along the direction of the incident light. Take T_{13} for example:

$$\begin{cases} x'_{T13} = x_{T13} + L_3 \cdot x_s \\ y'_{T13} = y_{T13} + L_3 \cdot y_s \\ z'_{T13} = z_{T13} + L_3 \cdot z_s \end{cases} \quad (14)$$

(v) Euler frame conversion was used to convert the projected coordinates into the coordinates of the plane 2 coordinate system. The conversion formula is:

$$\begin{bmatrix} x' \\ y' \\ z' \end{bmatrix} = R\begin{bmatrix} x \\ y \\ z \end{bmatrix} - R\begin{bmatrix} x_0 \\ y_0 \\ z_0 \end{bmatrix} \quad (15)$$

$$R = \begin{bmatrix} u_x & u_y & u_z \\ v_x & v_y & v_z \\ n_x & n_y & n_z \end{bmatrix} \quad (16)$$

Among it, (x,y,z) is the original coordinate system coordinate, and (x',y',z') is the converted coordinate system coordinates. (x_0,y_0,z_0) is the coordinate origin in the original coordinate system after conversion. (u_x,u_y,u_z), (v_x,v_y,v_z) and (n_x,n_y,n_z) is the unit vector of the converted coordinate system axes. Take T_{13} for example, after conversion, the axes x and y axes are respectively $\frac{T_{22}-T_{21}}{|T_{22}-T_{21}|}$ and $\frac{T_{24}-T_{21}}{|T_{24}-T_{21}|}$. Then project each vertex of heliostat 1 to the plane of heliostat 2, as schematic diagram is shown in Figure 6.

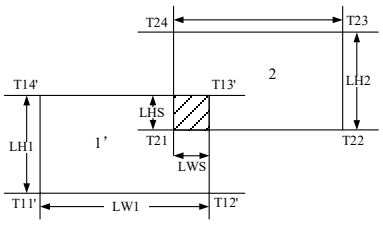

Figure 6. Schematic representation of the overlap rate

(vi) The horizontal and vertical edges of the overlapping area can be represented as:

$$\begin{cases} LW_S = LW_1 + LW_2 - (max(x_{T12}, x_{T22}) - min(x_{T11}, x_{T21})) \\ LH_S = LH_1 + LH_2 - (max(y_{T14}, y_{T24}) - min(y_{T11}, y_{T21})) \end{cases} \quad (17)$$

When LW_S or LH_S is less than or equal to 0, the overlap rate is 0, otherwise the overlap rate is $\frac{LW_S \times LH_S}{LW_2 \times LH_2}$. It can be seen that when the overlap rate is not 0, the shadow loss caused by heliostat 1 to mirror 2 is:

$$\eta_{sl} = \frac{LW_S \times LH_S}{LW_2 \times LH_2} \quad (18)$$

Thus, the shadow occlusion efficiency for all heliostats is:

$$\eta_{sb} = 1 - \sum \Delta\eta_{si} - \sum \Delta\eta_{bk} \quad (19)$$

Among it, $\Delta\eta_{si}$ is the shadow loss of the i-sided heliostat, and $\Delta\eta_{bk}$ is the block loss of the i-sided heliostat.

3.5. Overflow Efficiency

Overflow efficiency is also known as truncation efficiency, and the main reason for its existence is that all the solar light reflected by the heliostat cannot be fully absorbed by the collector. Because the tapered light of the sun has a non-negligible impact on the calculation of the truncation efficiency, the sun's light can not be regarded as a parallel light here. The truncation efficiency is the ratio of the solar radiation energy on the collector to the reflected solar light energy of the heliostat, which is affected by the tracking error of heliostat, light scattering and solar shape. According to reference [3], the energy flow density of the heliostat received on the surface of the heat suction tube is regarded as a Gaussian function. Therefore, the truncation efficiency is:

$$\eta_{trunc} = \frac{1}{2\pi\delta_{tot}^2} \iint \exp\left(-\frac{(x')^2+(y')^2}{2\delta_{tot}^2}\right) dx'\, dy' \quad (20)$$

Among it, δ_{tot} is the total standard error, and the hub point of the collector is (x', y').It is the total standard error.

δ_{tot} is the total standard error, which includes the solar shape deviation δ_{sun}, beam mass deviation δ_{bq}, Scattering effect δ_{ast}. Tracking error δ_t and δ_s are the standard deviation of the slope error. Their relationship is:

$$\delta_{tot} = \sqrt{D^2(\delta_{sun}^2+\delta_{bq}^2+\delta_{ast}^2+\delta_t^2)} \quad (21)$$

The relation of each parameter is:

$$\begin{cases} \delta_{bq}^2=(2\delta_s)^2 \\ \delta_{ast}=\frac{\sqrt{0.5(H_t^2+W_s^2)}}{4D} \\ H_t = \sqrt{LW \cdot LH}\left|\frac{D}{f} - cos\omega\right| \\ W_s = \sqrt{LW \cdot LH}\left|\frac{D}{f}cos\omega - 1\right| \end{cases} \quad (22)$$

Among it, f is the focal length, when the heliostine focus length is in the tilt range. When the heliostat focus length is in the tilt range, D is equal to f. $cos\omega$ refers to the cosine value of the unit vector of the incident light and the mirror axial normal vector. As shown in the reference [2], δ_{sun} is equal to 2.51mrad. For the SENER heliostat, δ_s is equal to 0.94mrad and δ_t is equal to 0.63mrad.

In conclusion, the optical efficiency of the heliostat is:

$$\eta = \eta_{sb}\eta_{cos}\eta_{at}\eta_{trunc}\eta_{ref} \quad (23)$$

Therefore, the annual average optical efficiency of the helostat is:

$$\eta_{year\_average} = \sum_i^N \sum_j^{365} \frac{\eta_{ij}}{N} \quad (24)$$

Among it, N is the total number of heliostats, and i is the i-sided heliostat, and j is the j-sided month.

The output thermal power of the heliostat field is:

$$E_{field} = DNI \cdot \sum_i^N A_i\eta_i \quad (25)$$

Among it, $A_i = LW \cdot LH - LW_s \cdot LH_s$ is the lighting area of the i-sided heliostat. η_i is the optical efficiency of the i-sided mirror. DNI is the normal direct radiation irradiance, whose expression is:

$$DNI = G_0[a + bexp(-\frac{c}{sin\alpha_s})] \quad (26)$$

$$\begin{cases} a = 0.4237 - 0.00821(6 - H)^2 \\ b = 0.5055 + 0.00595(6.5 - H)^2 \\ c = 0.2711 + 0.01858(2.5 - H)^2 \end{cases} \quad (27)$$

Among it, G_0 is the solar constant which is equal to 1.366kW/m2, and H is the altitude of the heliostat field.

Therefore, the average annual output thermal power of the heliostat field:

$$E_{year\_average} = \sum_j^{12} \frac{E_{field\_j}}{N} \quad (28)$$

Average annual output thermal power per unit mirror area of the heliostat field:

$$E_{area\_year\_average} = \sum_j^{12} \frac{E_{field\_j}}{N \cdot LW \cdot LH} \quad (29)$$

4. Model Solution of Calculation For the Efficiency Parameters

In order to have a clearer understanding of the distribution and characteristics of the heliostat field in problem 1, the mirror field distribution map in problem 1 is drawn as follows:

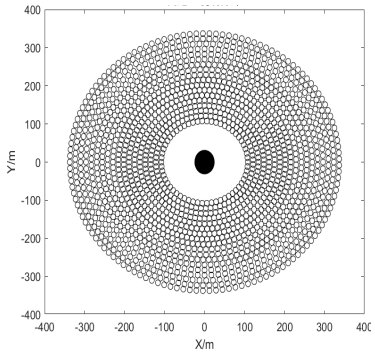

Figure 7. Mirror field distribution in the first part

4.1. Distribution Law of The Cosine Efficiency

The calculation of the cosine efficiency in the tower heliostat field field is the most critical, because it has the highest loss ratio, and the cosine efficiency is obviously different with the four seasons. Now, the four dates of March 21, June 21, September 21 and December 21 are used to draw the cosine efficiency distribution map as follows:

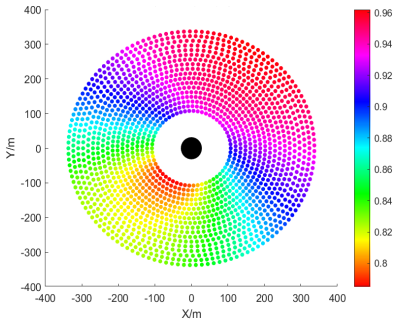

Figure 8. Cosine efficiency distribution on March 21st

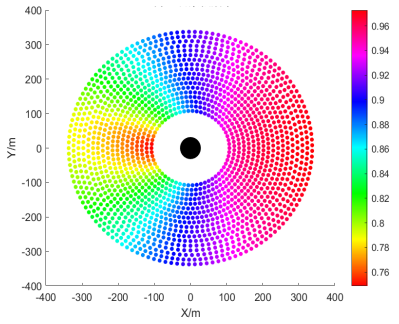

Figure 9. Cosine efficiency distribution on June 21st

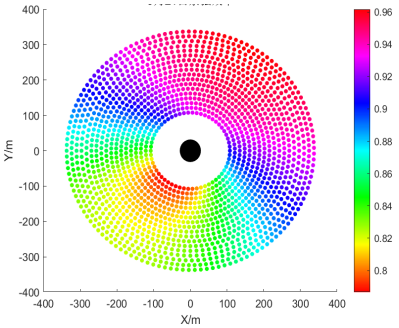

Figure 10. Cosine efficiency distribution on September 21st

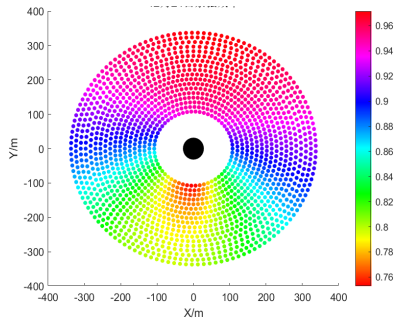

Figure 11. Cosine efficiency distribution on December 21st

4.2. Distribution pattern of the atmospheric transmission rate

From the formula of atmospheric transmission, it is not difficult to see that the magnitude of the atmospheric transmission efficiency is inversely proportional to the distance:

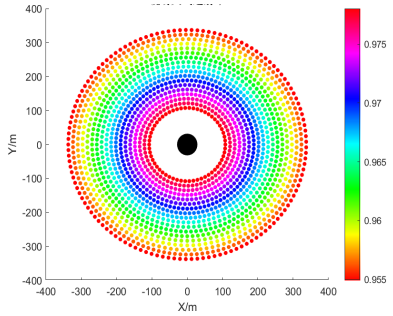

Figure 12. Atmospheric transmission efficiency

4.3. Shadow occlusion efficiency

The shadow occlusion efficiency can be effectively improved by optimizing the distribution of the mirror field.

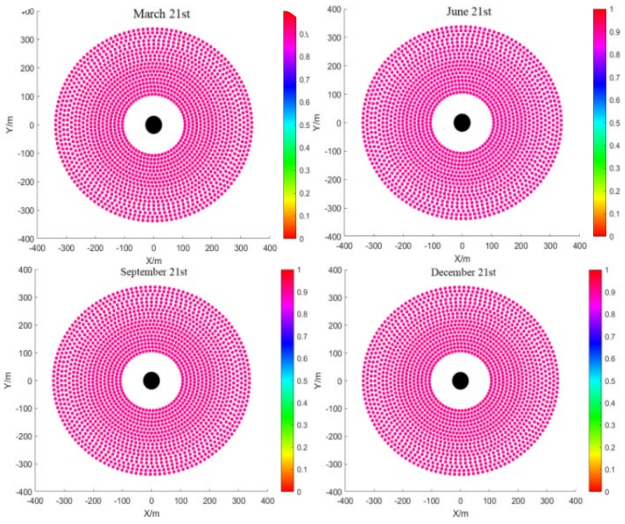

Figure 13. Shadow occlusion efficiency for the four representative dates

4.3. Integrated Optical Efficiency

The comprehensive optical effects of March 21, June 21, September 21 and December 21 are shown as follows:

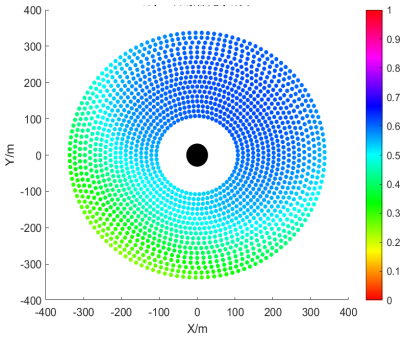

Figure 14. Optical efficiency distribution on March 21

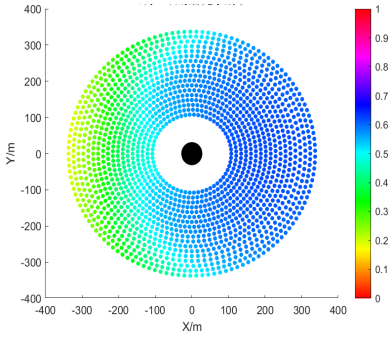

Figure 15. Optical efficiency distribution on June 21

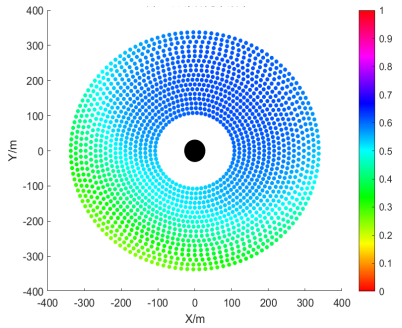

Figure 16. Optical efficiency distribution on September 21

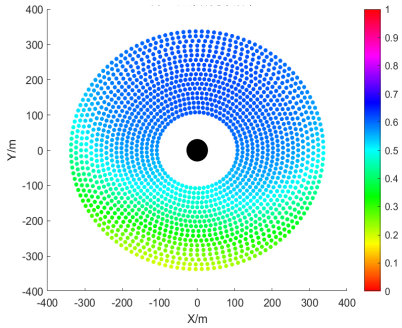

Figure 17. Optical efficiency distribution on December 21

In the previous mathematical model, the average optical efficiency, average cosine efficiency, average occlusion efficiency and average truncation efficiency can be calculated on the 21st day of each month.The average local five time periods on the 21st of each month, traversed for 12 months, and put it into the first part of the model. The annual average optical efficiency and output power table are shown in the table.Average annual optical efficiency is 0.6696; average annual cosine efficiency is 0.7564; annual average shadow occlusion efficiency is 0.9766; average annual truncation efficiency is 0.9975; average annual output thermal power is 35539.1747W; mean annual output thermal power per unit area is 0.5657W.

4.3. Modelling Verification

In the model one-truncation efficiency index, it is considered that the energy flow distribution of the sun-reflected solar ray on the collector is approximated by the Gaussian distribution. According to the problem, the distribution of a single helophoscope reflected to the collector surface is shown in Figure 17.The distribution of spot energy flow is Gaussian, The hypothesis is confirmed.

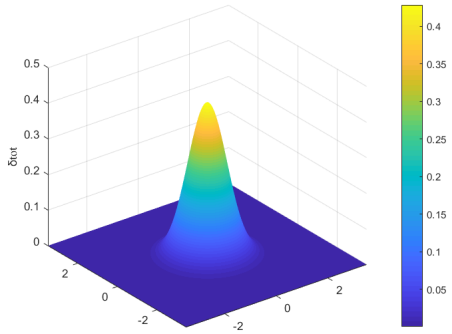

Figure 18. Optical efficiency distribution on December 21

5. Mirror Field Distribution and Optimized Model Building and Solution

5.1. Limit The Case of The Constraints

Establish a single objective optimization model, the objective function is to maximize the maximum annual average output thermal power per unit mirror area; the decision variables are the mirror width, the mirror height, the installation height and the position coordinates of the absorption tower; the constraints are the size range of the helioscope and the coordinate range of the absorption tower

For this single-objective optimization model, this paper applies the five-dimensional spatial particle swarm algorithm to solve, the algorithm flow diagram is shown below.

- STEP 1: Set the population parameters: the initial population number is 100, the spatial dimension is 5, and the maximum number of iterations is 100.
- STEP 2: Set position parameter limits and speed limits.
- STEP 3: set the inertia weight to 0.8, self-learning factor 0.5, and group learning factor 0.5.
- STEP 4: Generates the initial population, first randomly generates the initial population location, then randomly generates the initial population speed, then initializes the best position of the individual history, and the best fitness of the individual history, and finally initializes the best position of the group history, and the best fitness of the group history.
- STEP 5: The particle swarm algorithm iteration starts
- STEP 7: Update the speed and perform the boundary process of the speed.

- STEP 8: Update the location and perform a boundary process on the position.
- STEP 9: Conduct the adaptive variation.
- STEP10: Judge the constraint conditions and calculate the fitness of each individual position in the new population.
- STEP11: Comparing new fitness with individual history.
- STEP12: Comparing the best fitness of individual history with the best fitness of population history.
- STEP13: Repeat the cycle of STEP 5 ~ STEP12 until the iteration number reaches 100 and ends the cycle.
- STEP14: Output the results and the charts.

According to the results, it is found that many heliostats have low power values. On the premise of satisfying the average annual output power and the rated power of 60MW, these points with low power values can be eliminated.

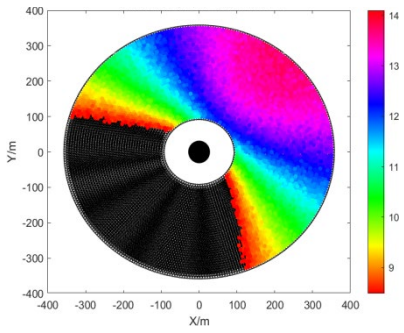

Figure 19. Power distribution after optimized again

5.2. Different Eyepiece Sizes

The objective function is unchanged, and the heliostatic scope size in the constraint is no longer a uniform value but can be different quantities, Because the size of the heliostat is no longer uniform, we adopted the chromosomal encoding mode of the genetic algorithm.

The optimal solution after the initial optimization of the algorithm is that the total number of mirror fields is 6,384 pieces, and the average annual output power per unit area is 530.6W.

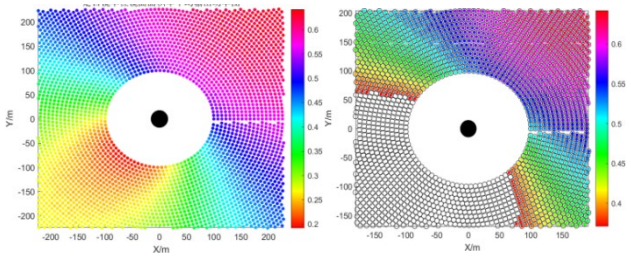

Figure 20. Power efficiency distribution map before and after optimization

6. Model Analysis and Evaluation

6.1. Model Analysis

For the model used in problem one, when calculating the normal direct radiation irradiance DNI, it ignores the different altitude caused by the uneven terrain, which leads to the error of the normal direct radiation irradiance. In addition, the mirror reflectivity is greatly affected by the mirror area dust, and selecting the mirror reflectivity constant will also bring some error.

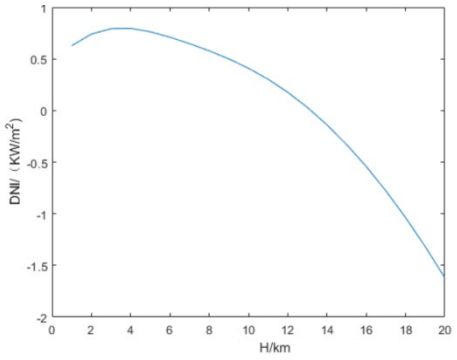

Figure 7. The relationship curve between the irradiance of the normal direct radiation and the altitude

For the models of problem two and problem three, since the genetic algorithm and the particle swarm optimization algorithm are solved through iteration, the initial population size and the number of iterations will greatly affect the formation of the solution. In addition, the selection of the initial population is also very important, which can avoid the generation of local optimal solution to a certain extent.

6.2. Model Evaluation

Single-objective optimization model has several advantages or disadvantages as follows: easy to solve; results consistency; the degree of abstraction of the problem is relatively high; sensitive to initial conditions.

Particle population algorithm has several advantages or disadvantages as follows: strong global optimization ability; the principle is relatively simple; search ability; High requirements for parameter setting; Easy to fall into a dimension disaster.

Genetic algorithm has several advantages or disadvantages as follows: Wide range of application; Strong parallel processing capability; The global optimal solution can be found; Strong ability to handle constraints; A large number of computing resources are needed; It is difficult to set parameters; May be trapped by the local optimal solution; Long running time.

For the local optimal solution, the particle swarm algorithm can be improved by some ways, such as the chaotic particle swarm algorithm for optimization, the chaotic particle swarm algorithm introduces the chaos theory into the particle swarm algorithm. By introducing chaotic mapping to increase the randomness of the search space improves the global search capability of the algorithm.

7. Conclusions

In this paper, we calculate and optimize the tower heliostat field by using single objective optimization, high-dimensional particle swarm algorithm and multiple group genetic algorithm. Based on the actual data, the calculation is processed with the model. At the end of the article, the advantages and disadvantages of the model and the algorithm are also analyzed, and the model verification is conducted. Finally, we conduct a comprehensive evaluation of the proposed model: the model of this paper can reasonably solve the problem and has strong practicability and high efficiency, but high dimensional particle swarm algorithm due to easily get local optimal solution, so can introduce the chaotic mapping to increase the randomness of the search space, improve the global search ability of the algorithm.Through the research and improvement of the tower heliostat field, the development of solar energy utilization technology and even other part of technology can be promoted.

Acknowledgements

This research did not receive any specific grant from funding agencies in the public, commercial, or not-for-profit sectors.

References

[1] Zhang Ping, optical efficiency of solar tower [J], Technology and Market, 2021,28 (6): 5-8.

[2] Song Haixiang. Study on the influence of dust accumulation on heliostat reflectance and measurement method [D]. Hangzhou: China Jiliang University, 2021.

[3] Badescu V. Theoretical derivation of heliostat tracking er rors distribution[J]. Solar Energy

[4] O. Farges, J.J. Bezian, M. El Hafi, Global optimization of solar power tower systems using a Monte Carlo algorithm: Application to a redesign of the PS10 solar thermal power plant [J], Renewable Energy, 2018, 119:345-353.

[5] Li Qiming, Zheng Jiantao, Xu Haiwei, Liu Mingyi, Pei Jie, Liu Guanjie. Discussion on solar thermal power generation in Xizang province [J]. Journal of Solar Energy, 2012 (s1), 57-62.

[6] Guo Su, Liu Deyou, Zhang Yaoming. Solar thermal power generation series articles (5) —— tower solar thermal power generation helioscope [J]. Solar energy, 2006, (5): 34-37.

[7] Wang Jun, Zhang Yaoming, Liu Deyou, Sun Liguo, an Cuicui. Solar thermal power generation series articles (8) Slot solar thermal power generation DSG technology [J]. Solar energy, 2007, (2): 26-27.

[8] Yuan Jianli, Lin Rumou, Jin Hongguang, Han Wei, Hong Hui. Solar thermal power Generation System and Classification (Part A) [J]. Solar energy, 2007, (4): 29-32.

[9] Zhang Yaoming, Zhang Wenjin, Liu Deyou, Sun Liguo, Liu Xiaohui, Wang Jun. Solar thermal power generation series article (17) Research and development of 70kW tower solar thermal power generation system (below) [J]. Solar energy, 2007, (11): 17-40.